IOPscience iopscience.iop.org

Home Search Collections Journals About Contact us My IOPscience

Mechanical characterization of C_{60} whiskers by MEMS bend testing

This article has been downloaded from IOPscience. Please scroll down to see the full text article.

2009 J. Phys.: Conf. Ser. 159 012006

(http://iopscience.iop.org/1742-6596/159/1/012006)

The Table of Contents and more related content is available

Download details:
IP Address: 155.198.134.118
The article was downloaded on 14/04/2010 at 11:28

Please note that terms and conditions apply.

Journal of Physics: Conference Series **159** (2009) 012006 doi:10.1088/1742-6596/159/1/012006

Mechanical characterization of C_{60} whiskers by MEMS bend testing

MP Larsson and S Lucyszyn

Optical and Semiconductor Devices Group
Department of Electrical and Electronic Engineering, Imperial College London, Exhibition Road, London, SW7 2AZ, UK

E-mail : s.lucyszyn@imperial.ac.uk

Abstract. Little has been published on the mechanical characteristics of C_{60} whiskers, due to the inherent difficulties in physically mounting such small test samples. Earlier reported results suggested Young's modulus values of 32 and 54 GPa, with 130 and 160 nanometer diameter C_{60} whiskers, respectively, using compressive deformation techniques. In our work, an experimental bespoke silicon-based microelectromechanical system has been developed to extract another value. It has been found, through parameter extraction techniques, that a Young's modulus of only ~ 2 GPa is obtained with a C_{60} whisker having a diameter of 4 microns. By including the previously published data points, there is now strong evidence to suggest an inverse proportionality relationship between the Young's modulus and the diameter of a C_{60} whisker.

1. Introduction

Since the discovery of fullerene C_{60}, by Kroto *et al.* [1], advances in the field of fullerene chemistry have led to a number of interesting developments, such as the carbon nanotube (CNT). The C_{60} molecule consists of carbon atoms located at the nodes of a series of hexagons and pentagons arranged in a cage lattice, defined by alternating double and single bonds. In contrast to CNTs, which can be visualised as rolled-up sheets of graphene, C_{60} whiskers contain no long-range hollow structure. Instead, structural characterisation has indicated the whiskers are solid, consisting of a series of C_{60} molecules, bound through a combination of van der Waals interactions and chemical bonds. The latter suggests that C_{60} whiskers contain chains of polymerised C_{60} within their structure. A transition from a poly- to single-crystalline structure may occur when the diameter of C_{60} whiskers decreases to approximately 1 μm [2-3]. The absence of grain boundaries, combined with the observation of enhanced intermolecular bonding, are the main reasons why C_{60} nanowhiskers are expected to exhibit superior electrical and mechanical properties to those of their larger-diameter counterparts.

In recent years, work at the University of Tsukuba and National Institute for Material Science (both in Tsukuba, Japan), has led the way in determining the mechanical properties of C_{60} nanowhiskers using compressive deformation techniques [4]. Asaka *et al.* determined Young's modulus values of 32 and 54 GPa, with 130 and 160 nanometer diameter C_{60} whiskers, respectively. This is in excess of the 8.3 to 20 GPa range that they reported in their survey for bulk crystal C_{60} [4].

© 2009 IOP Publishing Ltd

At Imperial College London, work on the electrical and mechanical characterization of C_{60} whiskers and nanowhiskers was undertaken within a two-year research programme [5-6]. Within this activity, a bespoke microelectromechanical systems (MEMS) electrothermal 4-point bend tester was developed for the mechanical characterization of C_{60} (nano)whiskers, for operation under an optical microscope. The characterization of Young's modulus, using the results from one of the experiments, will be investigated here.

2. Growth of C_{60} whiskers

C_{60} molecules are known to polymerise under high temperature [2-3], high pressure conditions and in the presence of ultraviolet (UV) radiation. Relatively recently, Miyazawa *et al.* reported a technique for growing needle-like structures of C_{60} from solution at room temperature. A logical first stage for our research was to reproduce the results [5] of Miyazawa *et al*. Here, the needles of C_{60} grew in arbitrary directions through a process of liquid-liquid interfacial precipitation (LLIP), between C_{60} saturated toluene and isopropyl alcohol (IPA), as shown in figure 1(a). Diameters ranged from hundreds of nanometres to several microns, with lengths reaching several hundreds of microns. Needles with diameters below 1 μm are referred to as C_{60} nanowhiskers, and those with larger diameters are described as C_{60} whiskers, both seen in figure 1(b). The DC characterisation of such samples has been recently reported [6].

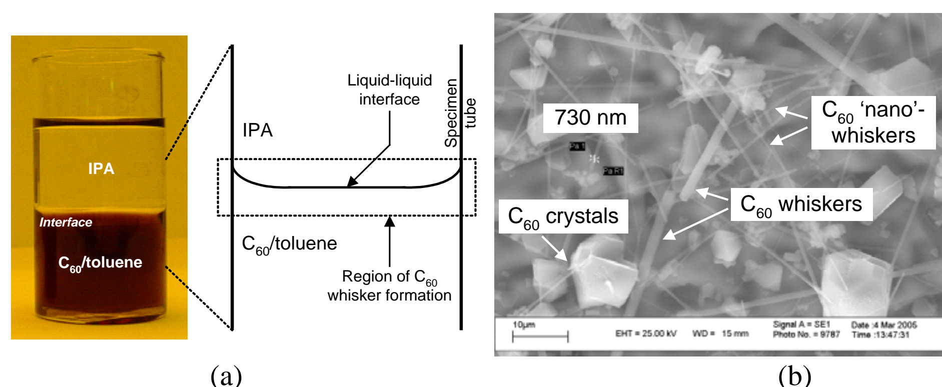

Figure 1. Miyazawa's liquid-liquid interface growth technique: (a) growth vial indicating the region in which C_{60} whiskers are observed to grow in an ad hoc manner; and (b) products found within the liquid-liquid interface following several hours of growth. (Reproduced by permission of The Electrochemical Society. [6])

3. Mechanical bend testing

At the time of this work, no mechanical characterisation on C_{60} nanowhiskers had been reported in the open literature. However, relatively recently, the Young's modulus (E) of a C_{60} nanowhisker was ascertained from a buckling test in a transmission electron microscope (TEM), using a probe tip with position control and force-feedback [4]. Techniques for determining the mechanical properties of CNTs, in particular, have been widely reported in the open literature. The most common involves tensile loading using the tip of an atomic-force microscope (AFM) probe [7]. In such situations, the CNTs are either attached to the AFM tip by pressure contact or they are grown on. The former is more common; nevertheless, non-ideal attachment between CNT and the substrate and tip of the AFM limit the accuracy of the data obtained. The problem of gripping can be avoided by reversing the loading direction of the AFM tip and performing a buckling test. With this approach, the point of loading shifts during the test; once again invalidating the results. Problems with sample gripping or loading during mechanical testing can be resolved through the use of bend tests. Such tests are popular in mechanical engineering, for the characterisation of brittle materials. In such cases, 3- and 4-point tests are employed by convention, and the deflection and fracture data can be used to determine E and fracture strength; which for brittle materials is known as the modulus of rupture (MOR).

Micromachined tensile testers have successfully been developed for the characterisation of materials commonly used in MEMS technology, such as silicon and polysilicon. These devices are quite sophisticated, incorporating either electrothermal or electrostatic actuation. Force feedback can be achieved using electrostatic comb-drive sensors. It is the successful application of such devices that is the inspiration behind the mechanical testing of C_{60} (nano)whiskers. As C_{60} whiskers are large enough to be observed under an optical microscope, this lends itself well to the use of simplified MEMS mechanical testers, to evaluate their deflection and fracture characteristics.

3.1. MEMS bend tester

A MEMS electrothermal bend tester was designed for use under an optical microscope. The design was based around the dimensions and likely deflection range of a typical C_{60} (nano)whisker. Figure 2 illustrates the proposed device, containing a pair of back-to-back bend testers on a common die.

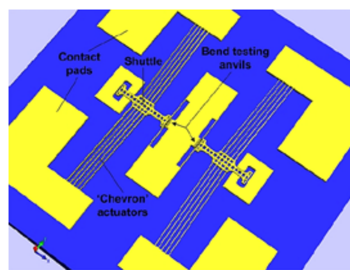

Figure 2. Proposed MEMS bend tester, designed for C_{60} (nano)whiskers.

Actuation is achieved by application of current between pairs of contact pads, causing heating within 'chevron' arms that supports a suspended 'shuttle' structure. The arms are angled in a manner to generate linear motion from their combined thermal expansion. The shuttle is attached to a set of anvils at one end, which are close to a fixed set of anvils (opposite), in order to apply bending point loads on a pre-positioned C_{60} whisker sample.

A process flow for the fabrication of the MEMS structure is shown in figure 3, relying on a two-stage deep reactive-ion etching (DRIE) of a bonded silicon-on-insulator (BSOI) wafer, to form an interdigitated set of (movable) anvil and (fixed) platform structures. Such features are important to support and raise the C_{60} (nano)whisker from the clearance zone between device and handle silicon layers, such that they can be loaded without falling into, and getting trapped within, the clearance area.

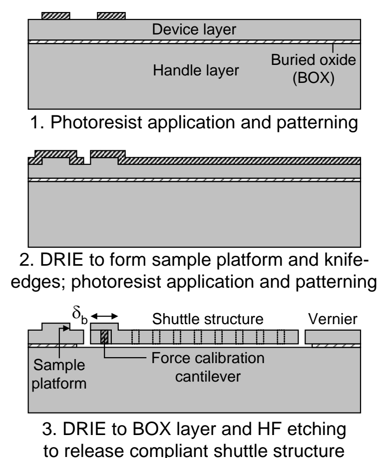

Figure 3. Process flow outlining key steps in the fabrication of the MEMS bend tester.

Prototypes were fabricated to test device performance and compare this with design predictions. Figure 4 shows optical microscope images of a prototype MEMS bend testers.

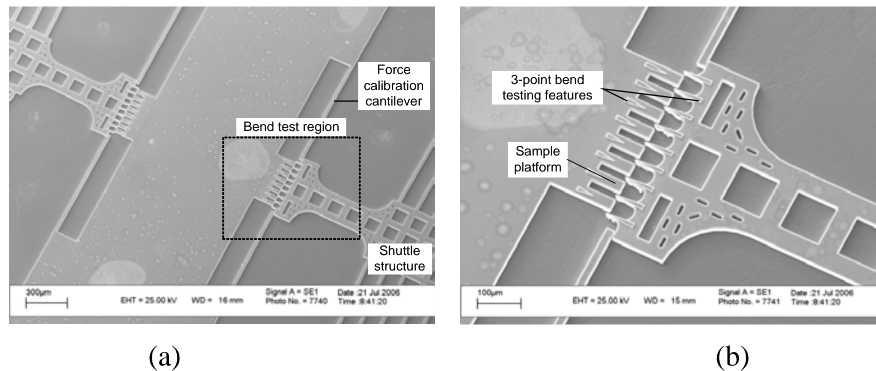

(a) (b)

Figure 4. Prototype MEMS bend testers: (a) central region showing both sets of loading anvils; and (b) detail over the region indicated in (a).

The MEMS bend tester was designed for ease of fabrication and use. To this end, features for rapid optical evaluation of force-deflection characteristics were included. Such features include a Vernier scale, with micron demarcations, and force calibration cantilevers to help in the determination of bending forces exerted on C_{60} (nano)whisker samples during testing. As the Young's modulus for silicon can be estimated to a good approximation, the force deflection characteristics for the cantilevers can be ascertained from their dimensions. Bend tests in the absence of samples will allow the deflection-force characteristics of the bend tester to be determined as a function of applied DC power. When a C_{60} (nano)whisker sample is inserted between the anvils, the force-deflection-power characteristic will change; the difference relative to the original being the additional force applied to the sample. This approach, although simple in theory and easy to realise in a MEMS device, can be difficult to achieve in practice. The problem lies in the ability to resolve differences in force-deflection-power characteristics, under an optical microscope, from normalised values after the insertion of a sample between the loading anvils. Even if quantitative data cannot be obtained, qualitative information on the mode of fracture and the extent of deformation prior to this would be useful information.

Bend testers with 5 and 10 supporting arms, either side of the central shuttle, were fabricated to vary the force applied to different samples. The spacing between opposite anvils was varied along each tester to accommodate whiskers of different diameters and lengths. Finally, testers with anvil arrangements to perform 3- and 4-point tests were designed. The latter allows more accurate data to be obtained, whereas the former generates greater observable deflections. The displacement performance of the prototype bend testers was evaluated by passing current in manner shown in figure 5(a). The thickness of the device layer in all prototypes was 10 μm, and resultant shuttle deflections-power densities are displayed in figure 5(b). For example, the graph shows that a 10-arm device produces a 12.5 μm/W deflection per Watt of applied DC power.

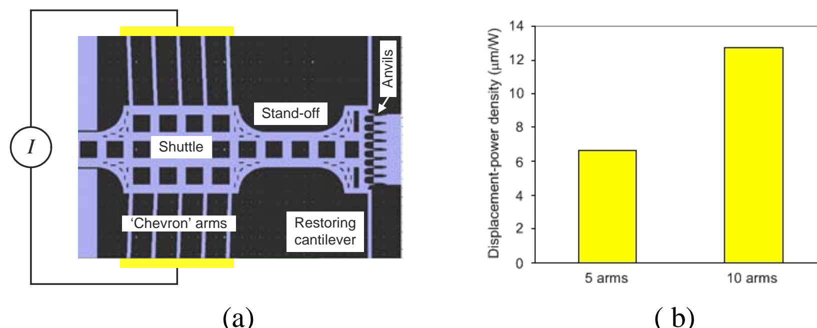

(a) (b)

Figure 5. (a) illustration showing the application of current to a tester; and (b) averaged deflection-power density data for devices with 5 and 10 arms on either side of the shuttle.

During performance evaluations, an infrared camera was used to image the thermal distribution throughout the device and measure its average temperature as a function of applied power. Figure 6 shows the variation in average device temperature with input power on a 10-arm bend tester. At full deflection, the device reaches a maximum temperature that is marginally in excess of 70 ^{o}C, corresponding to a power of approximately 2.7 W. Comparison between actual performance and design predictions revealed good agreement, showing the bend tester device to be functioning as intended. The next step involved the testing of real samples.

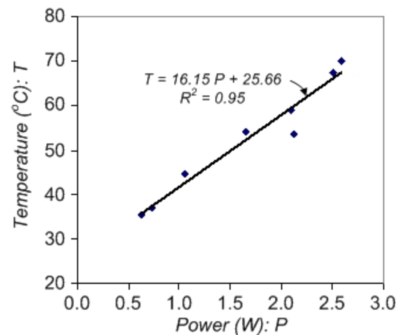

Figure 6. Variation in average die temperature with applied power.

3.2. Bend tests on C_{60} whiskers

The placement of C_{60} nanowhiskers between the anvils of the bend testers was always going to be difficult to achieve in practice. One approach adopted the direct application of a solvent-suspension of nanowhiskers over target areas. The disadvantage of this approach is that it is imprecise, and introduces 'debris' in the clearance zone between the movable shuttle and the substrate handle layer. Although the shuttle is capable of generating sufficient force to override such obstructions, the possibility of extracting *E* from a nanowhisker sample through differentials in force-displacement-power coefficients was not possible.

A more reliable approach for the precise positioning of C_{60} nanowhiskers in regions between the anvils of the bend testers was eventually employed. The technique involved the use of a flame-stretched glass capillary tube, having a tip diameter of 5 μm. By attaching the capillary tube to a Mitutoyo *x*-*y*-*z*-positioner, a high-resolution positioning device could be realised, as shown in figure 7. If two are used in parallel, C_{60} nanowhiskers can be moved into position with considerable ease.

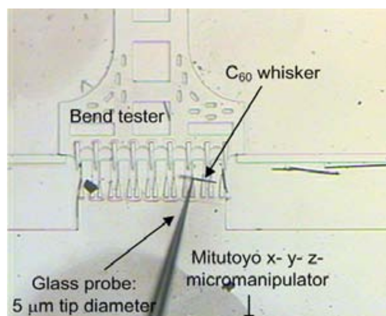

Figure 7. Placement of a C_{60} whisker between the anvils of a bend tester, using a micropositioner attached to a capillary tube having a 5 μm tip diameter.

In practice, the glass capillary tubes used were coated in a sputtered layer of Au, to maintain a clean contact surface and promote electrostatic attraction with nanowhiskers. It is known that Au surfaces give up electrons during rubbing contact, due to the triboelectric effect. This will allowed the capillary tubes to establish a positive static charge of sufficient magnitude to attract nanowhiskers, which have been shown to develop an attraction to positively charged surfaces. In some cases, this 'pick-n-place'

approach did not work, as van der Waal's forces between nanowhiskers and the silicon surface were too great. Such surface interactions tended to be greater with the narrowest nanowhiskers. In some cases, the nanowhiskers could be dislodged from the silicon surface using the probe tip; however, the difference in size between the two often caused the nanowhisker to fracture. As such, the narrowest nanowhiskers could not be successfully positioned using this technique, and only samples with diameters in excess of 0.5 μm could be placed between the anvils of the bend testers.

Optical microscope images of samples in 3- and 4-point bend testers are shown in figures 8 and 9, respectively. A fractured C_{60} nanowhisker is seen in figure 8(a), following a prior successful 3-point bend test. Failure appears to be entirely brittle, as no signs of plastic deformation are visible. Figure 8(b) shows the same tester during the application of DC power. The larger C_{60} whisker, to the right of the C_{60} nanowhisker, is now experiencing loading between the three contacting anvils. Repeated loading and unloading revealed elastic deformation characteristics. Unfortunately, in the process of this basic 'fatigue' test, the sample worked its way above the anvils and could not be tested to destruction.

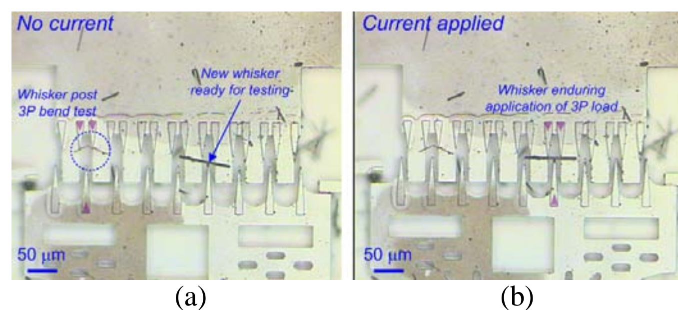

(a) (b)

Figure 8. 3-point bend test of C_{60} whiskers: (a) before; and (b) during tester actuation.

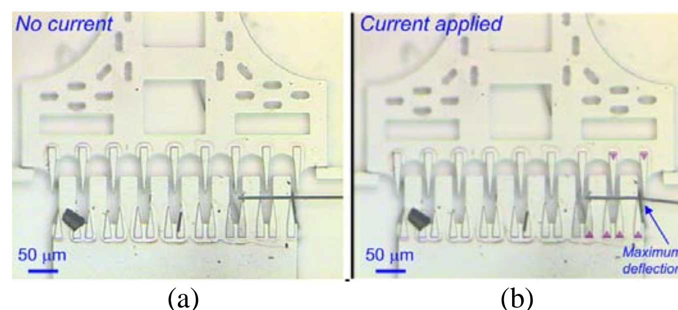

(a) (b)

Figure 9. 4-point bend test of a C_{60} whisker: (a) before; and (b) during tester actuation.

Closer inspection of the image in figure 9(b) reveals that the loading anvil at the far right of the tester is marginally longer than the other three anvils in contact with the whisker. So despite the fact that the whisker is clearly under load from all four anvils, the greatest deformation (and, hence stress) is occurring in the region above the third from the left anvil. The unusual situation conveniently produces what is in effect a cantilever bend test, with the 'fixed' support provided by anvils 1-3 (left to right), and the point load applied by the 4th anvil. Figure 10 shows a simplified schematic representation of the cantilever bend test between the 3rd and 4th anvils.

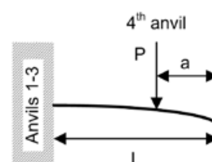

Figure 10. Cantilever bending due to a transverse point-load, representing a possible scenario for loading between anvils 3 and 4 of the bend tester in figure 9.

The governing equation that relates the deflection of the cantilever's tip is given by [8]:

$$\delta = \frac{P}{6EI}\left(2L^3 - 3L^2 a + a^3\right) \tag{1}$$

where δ is the tip deflection, I is the second moment of area of the cantilever, and P is the applied load. The image in figure 9(b) was captured at the instant immediately prior to sample fracture, which occurred at the 4th anvil. The deflection observed is the maximum for the sample prior to fracture. The distance between the 3rd and 4th anvils is approximately 10 μm, the maximum deflection noted at the point of load application was measured at just under 1.5 μm and the whisker's diameter was determined to be approximately 4 μm. Figure 11 shows the fractured whisker following successful bend testing. The fracture point indicates brittle failure.

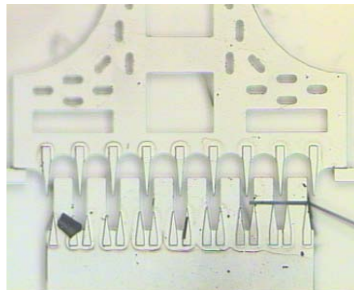

Figure 11. C_{60} whisker showing signs of brittle fracture following a bend test.

3.3. Experimental results

The resolution of the optical microscope and deflection measurement system used were not sufficient to allow representative load force data to be inferred from applied DC power, as initially envisaged. An approximation for the Young's modulus of the C_{60} whisker in figure 9 is given, assuming a maximum resolution for the optical system of 1 μm. If there is no change observed in the force-deflection-power characteristics of the bend tester, following sample insertion, the additional load force applied to the sample corresponds to that required to move the unloaded tester through a distance of ~ 1 μm. Based on the dimensions of the force calibration cantilevers and an assumed E for silicon of 160 GPa, this corresponds to a force of ~ 2.5 μN; in other words, the bend tester has a force-deflection characteristic of 2.5 μN/μm. Assuming this force to be of the same order of magnitude to the maximum load applied to the whisker in the bend test, a simple calculation using equation (1) yields an approximation of its stiffness and, hence, E. By assuming the whisker's shape to follow that of a solid rod of diameter, D, the second moment of area, I, is calculated using the following standard expression:

$$I = \frac{\pi D^4}{64} \tag{2}$$

Although the whisker's tip deflection is cropped from the image in figure 9(b), its value was measured, and with remaining measurements on the loaded sample inserted into equation (1), to yield a value of E ~ 2 GPa. This value is at least a factor of 10 lower than that reported by Asaka *et al.* [4], with their axially-loaded C_{60} nanowhisker having a diameter of 160 nm. Our C_{60} whisker has a diameter of 4 μm, which is at least 25 times thicker than those reported by Asaka *et al.* [4]. This makes it an interesting sample for comparison. From the limited experimental data available (two data points from Asaka *et al.* and one from our work), Young's modulus can be crudely modelled, as shown in figure 12.

Ideally, more data points from controlled samples are needed in order to determine a more definitive model, but the inverse proportionality of Young's modulus to C_{60} whiskers diameter is evident. This appears to contradict any notion of a fixed value of Young's modulus for C_{60} whiskers.

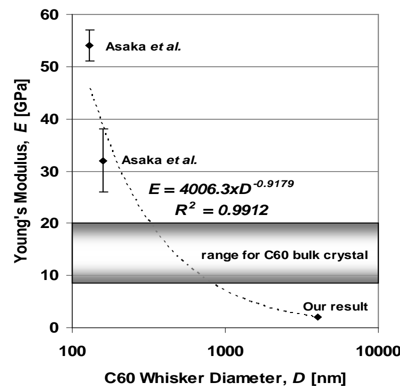

Figure 12. Characterization of Young's modulus with C_{60} whisker diameter.

4. Discussion and conclusions

The lower stiffness of the whisker characterised in this study is likely to be a consequence of the presence of grain boundaries due to its polycrystalline structure. Of course, another possibility is that the technique employed leads to an underestimate of the stiffness of the whisker. One possible source of error is the measurement of maximum whisker deflection prior to failure. Although previous deflections can equally be used to determine E, the final value was used as this facilitated measurement through the optical microscope. Other, more minor, errors may come from the approximation leading to the scenario represented by figure 10 and subsequent use of equation (1).

Despite the limitations of the mechanical characterisation carried out in this study, the results are informative on qualitative grounds as they provide evidence for brittle fracture in C_{60} nanowhiskers as well as larger diameter whiskers. Our parameter extraction method suggests a value for $E \sim 2$ GPa for a 4 μm diameter C_{60} whisker. By including the previously published data points, there is strong evidence to suggest an inverse proportionality relationship between the Young's modulus and the diameter of the C_{60} whisker.

Acknowledgements

The authors are very grateful to Dr Kun'ichi Miyazawa, for providing the initial inspiration for our work on C_{60} whiskers and ongoing discussions. We also like to thank the UK's Engineering and Physical Research Council for funding this research (under grant GR/S97019/01).

References

[1] Kroto H W, Heath J R, O'Brien S C, Curl R F and Smalley R E 1985 C_{60}: buckminsterfullerene *Nature* **318** 162-3
[2] Miyazawa K, Kuwasaki Y, Obayashi A and Kuwabara M 2002 C_{60} nanowhiskers formed by the liquid-liquid interfacial precipitation method *J. of Mat. Res.* **17** 83-8
[3] Miyazawa K, Kuwasaki Y, Hamamoto K, Nagata S, Obayashi A and Kuwabara M 2003 Structural characterization of C_{60} nanowhiskers formed by the liquid/liquid interfacial precipitation method *Surf. and Int. Ana.* **35** 117-20
[4] Asaka K, Kato R., Miyazawa K, Kizuka T 2006 Buckling of C_{60} whiskers *App Phys. Lett.* **89** 071912
[5] Larsson M P and Lucyszyn S 2005 Directed growth of C_{60} nanowhiskers for millimetre-wave detectors *Romanian J. of Inf. Sci. and Tech.* **8** 305-20
[6] Larsson M P, Kjelstrup-Hansen J and Lucyszyn S 2007 Dc characterisation of C_{60} whiskers and nanowhiskers *ECS Trans.* **2** 27-38
[7] Yu M F, Files B S, Arepalli S and Ruoff R S 2000 Tensile loading of ropes of single wall carbon nanotubes and their mechanical properties *Phy. Rev. Lett.* **84** 5552-5
[8] Young W C and Budynas R G 2002 Roark's formulas for stress and strain (McGraw-Hill International Edition)